

2004

A model for radiation interactions with matter

Carrie Beck

Follow this and additional works at: <https://commons.emich.edu/honors>



Part of the [Mathematics Commons](#)

Recommended Citation

Beck, Carrie, "A model for radiation interactions with matter" (2004). *Senior Honors Theses & Projects*. 100.

<https://commons.emich.edu/honors/100>

This Open Access Senior Honors Thesis is brought to you for free and open access by the Honors College at DigitalCommons@EMU. It has been accepted for inclusion in Senior Honors Theses & Projects by an authorized administrator of DigitalCommons@EMU. For more information, please contact lib-ir@emich.edu.

A model for radiation interactions with matter

Abstract

The intent of this project is to derive a realistic mathematical model for radiation interactions with matter. The model may be solved analytically, but I will also employ two computational methods, a finite difference method and a stochastic (Monte Carlo) method to gain insight into the physical process and to test the numerical techniques. Radiation interactions with matter constitute a large number of important scientific, industrial, and medical applications. This project will derive a model for the interaction of radiation with matter, which might allow one to compare different designs for shielding. It is also applicable in atmospheric physics in studying how light penetrates clouds, or in astrophysics in describing solar radiation piercing through stellar atmospheres, or as a medical tool for imaging or cancer treatment.

Degree Type

Open Access Senior Honors Thesis

Department

Mathematics

First Advisor

Professor Walter Parry

Keywords

Matter, Radiation, Stochastic models, Mathematical models

Subject Categories

Mathematics

A Model for Radiation Interactions with Matter

Carrie Beck

Professor Walter Parry, Sponsor

Department of Mathematics

Eastern Michigan University

College of Arts and Sciences

Fall Semester, 2004

Contents

1	Introduction	4
2	Theory	7
2.1	Physical Problem Description	7
2.1.1	Model Derivation	12
2.1.2	Discussion	17
2.2	Deterministic Modeling	18
2.3	Stochastic Modeling	22
2.4	Test Problems	29
3	Results	30
3.1	Analytical Solution	30
3.2	Data Analysis	33
3.2.1	Finite Difference	34
3.2.2	Monte Carlo	36
4	Conclusions	38
	Bibliography	39

List of Figures

2.1	Problem geometry	8
2.2	Particle sources: boundary $\psi_j^b(t)$ and interior $q(x, t)$	10
2.3	Discretization scheme for finite difference method	19
2.4	Illustration of knowns (circled) and unknowns for the k th interval	21
2.5	Flow chart of Monte Carlo algorithm	27
3.1	Test problem, $c = 0.1$	35
3.2	Test problem, $c = 0.5$	35
3.3	Test problem, $c = 0.99$	36

List of Tables

2.1	Parameters used for test problems	29
3.1	Analytical solutions for the test problem	33
3.2	Results of the deterministic solutions for the test problem	34
3.3	Results of the Monte Carlo solutions for the test problem	37
3.4	Statistical accuracy of the Monte Carlo solutions for the test problem	37

Chapter 1

Introduction

The intent of this project is to derive a realistic mathematical model for radiation interactions with matter. The model may be solved analytically, but I will also employ two computational methods, a finite difference method and a stochastic (Monte Carlo) method to gain insight into the physical process and to test the numerical techniques. Radiation interactions with matter constitute a large number of important scientific, industrial, and medical applications. This project will derive a model for the interaction of radiation with matter, which might allow one to compare different designs for shielding. It is also applicable in atmospheric physics in studying how light penetrates clouds, or in astrophysics in describing solar radiation piercing through stellar atmospheres, or as a medical tool for imaging or cancer treatment.

Radiation falls into two categories: charged particles and neutral particles. This project is primarily concerned with neutral particles, specifically neutrons and gammas. A neutron is one of the two fundamental particles that make up the nucleus of the atom and a gamma particle is a highly energetic photon. The physics of neutral particle transport is intimately connected with direct interac-

tions between the particle and its medium, whereas charged particles experience indirect forces. It is therefore a straightforward task to develop a mathematical model to describe the transport of neutral particles through a medium based on the physics of particle interactions. To derive the model, several assumptions [1] are made:

1. Particles are considered as points.
2. Particles may change direction only in a collision event.
3. Particle-particle interactions are neglected.
4. Collisions are considered as instantaneous.
5. All possible scatter directions of flight are equally likely.
6. There are a large enough number of particles that only the mean value is considered.

This project will employ two further simplifications; it will be in one dimension, and it will occur in a homogeneous medium. While this may seem limiting, it is still an involved process to obtain the model and the model is often used to obtain first order estimates in typical shielding and health physics applications. Once obtained, it is possible to directly solve the governing equations using analytic methods. In most real world applications, three dimensions must be taken into account, as should heterogeneous effects. However, it is impossible to solve these problems by hand and one must resort to computational methods, either deterministic or stochastic. In a deterministic method one usually discretizes the variables of interest and seeks the average solution in each interval. One such method is the finite difference method that will be utilized in this project.

In a stochastic method one uses physical information to determine probabilities of interaction of particles in the medium. One then proceeds by following a particle through the system to obtain a guess of the parameter of interest (for instance, transmission probability). This process can be repeated a large number of times to obtain an average of the parameter of interest and its associated uncertainty. The uncertainty will decrease as the number of followed particles increases. This project will employ all three methods so that one can verify the three solutions are the same and contrast the advantages and disadvantages of each.

Chapter 2

Theory

The first task is to make some definitions and some more explicit assumptions to formulate the problem physically and mathematically. After this will be a discussion as to how to model the problem computationally from a deterministic and stochastic standpoint.

2.1 Physical Problem Description

What follows is an elaboration an interview I had with Professor Edward Larsen of the University of Michigan, who is to be my graduate advisor once I complete my studies at Eastern Michigan University. upon graduation. The central topic of this project is actually due to him, and he has been very helpful with regard to clarifying the topics in this description.

First, it is illustrative to consider the problem geometry; it is provided in Figure 2.1. We are considering neutral particle transport through a semi-infinite block; the only finite direction extends from $0 < x < X$. In the other two (y, z) directions, the block is considered to be infinite. This is known as planar geometry

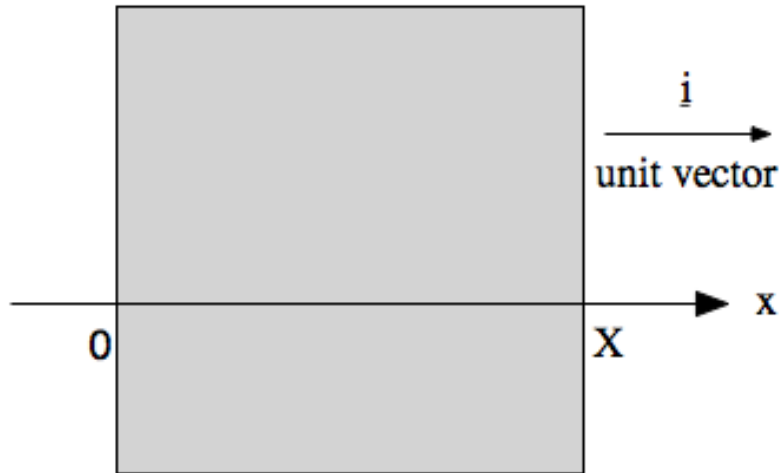


Figure 2.1: Problem geometry

in practice. Furthermore, we are only considering particle travel in the left and right directions. That is, if we designate $\underline{\Omega}$ as the particle direction, then $\underline{\Omega}$ is only allowed to have the values $\underline{\Omega}_1 = \underline{i}$ and $\underline{\Omega}_2 = -\underline{i}$, where \underline{i} is the traditional unit vector in the x direction. Because of this restriction, this problem is also known as the “Rod” model for particle transport. While this may seem limiting, it is still an involved process to obtain the model, and the model is often used to obtain first order estimates in typical shielding and health physics applications. Also, considering the sizes and numbers typical of neutral particles, we consider them to be points.

We further assume that all particles travel with the same speed, v , which might be thought of as a suitable average speed of a distribution of “real” particles. Also, particles inside the system ($0 < x < X$) have an incremental probability of colliding per incremental distance traveled designated by Σ_t , the *total cross section*, which is specified as a material property of the system. The dimensions of Σ_t are inverse length (cm). In practice this quantity is found by multiplying

the number density of atoms (the number of atoms in a unit volume, $\#/cm^3$) by σ_t , the total cross section of a single atom, which has units of area (cm^2). Interestingly, the quantities σ_t and Σ_t are well-known to vary significantly with the particle's speed due to quantum mechanical effects; that is, the target area a given atom presents to a particle can be very different for different particle velocities. This is one of the factors that requires our single-velocity assumption. Since the number density of atoms is typically many orders of magnitude higher than the density of radiation particles, the probability of particle-particle interaction is very low; here we neglect it completely.

Once a particle undergoes a collision with an atom from the system, we assume that one of two events can happen: the particle either scatters from the atom with probability c , or the particle is permanently absorbed with probability $1 - c$. The probability c is commonly called the *scattering ratio*, and allows us to define the *scattering cross section* to be $\Sigma_s = c\Sigma_t$. This may be thought of as the incremental probability of a scattering event per incremental distance traveled. Once a particle scatters, we assume that it has an equal probability of traveling forward ($\underline{\Omega}_1 = \hat{l}$) or backward ($\underline{\Omega}_2 = -\hat{l}$); $p = \frac{1}{2}$. This is known as isotropic scattering (all outgoing directions are equally likely). We also assume that particles only change their direction in a collision event, and that these events may be considered to be instantaneous, both of which are true enough in practice. Away from an atom, neutral particles are affected only by gravity, which is a very small effect, while collision events take place on the order of femtoseconds.

It may happen that there is an interior source of particles in the slab; we define this feature by $q(x, t)dx$, the source rate ($\#/sec$) at which particles are introduced into the system in the interval $(x, x + dx)$ at time t . Accordingly

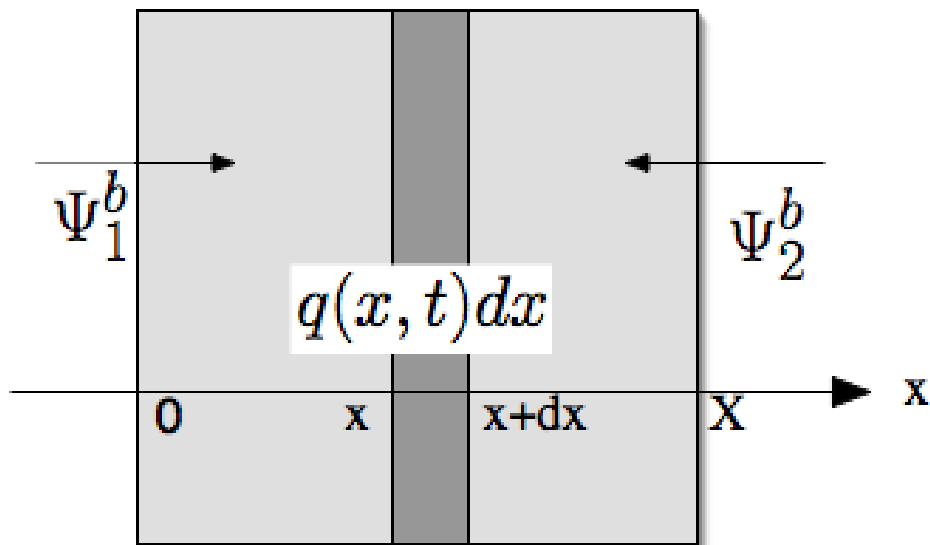


Figure 2.2: Particle sources: boundary $\psi_j^b(t)$ and interior $q(x, t)$.

$q(x, t)$ itself has dimension of (#/sec-cm). We assume that particles introduced by q have equal probability of traveling left or right. Typical problems of interest also include a prescribed boundary source. We designate these by $\psi_1^b(t)$, the rate (#/sec) at which right-traveling particles enter the system through the left boundary at time t , and $\psi_2^b(t)$, the rate (#/sec) at which left-traveling particles enter the system through the right boundary at time t . Figure 2.2 below depicts the nature of these source types.

With the quantities v , Σ_t , Σ_s , $q(x, t)$ and $\psi_j^b(x, t)$ specified, we may now proceed to develop the model. The main quantity of interest is given by $N_j(x, t)dx$, which is the number of particles traveling in direction $\underline{\Omega}_j$ ($j = 1$ or 2), located between x and $x + dx$ at time t . We are moving towards a system of coupled, differential equations that will relate $N_1(x, t)$ and $N_2(x, t)$ with corresponding initial and boundary conditions. The relationship will be developed based on physical principles using the quantities defined above. To begin, we first note

that $N_j(x, t)$ (without the dx) has units cm^{-1} so that we may interpret them as density functions. That is, for $0 \leq x_1 \leq x_2 \leq X$, we can use these functions to find:

$$\int_{x_1}^{x_2} [N_1(x, t) + N_2(x, t)] dx \quad (2.1)$$

to be the total number of particles (traveling in both directions) located between x_1 and x_2 at time t . Next we note that in an incremental time dt , each particle must travel a distance $ds = vdt$. Then, by the definition of the total cross section, $\Sigma_t = \frac{dp}{ds} = (\frac{1}{ds}$ times the incremental probability that in travelling a distance ds , a particle undergoes a collision). So we find that during an incremental time dt , each particle has the incremental probability $dp = \Sigma_t ds = \Sigma_t v dt$ of colliding with an atom. Putting this all together, we find that $dp N_j(x, t) dx = \Sigma_t v N_j(x, t) dx dt$ is the number of particles traveling in direction $\underline{\Omega}_j$ in the interval $(x, x + dx)$ that will undergo a collision during the time interval $(t, t + dt)$. Dividing through by dt , we get

$$\Sigma_t v N_j(x, t) dx = \text{the collision rate for } j\text{-particles in } (x, dx) \text{ at time } t \quad (2.2)$$

where j -particles should be understood to mean “particles traveling in direction $\underline{\Omega}_j$ ”, $j = 1$ or 2 .

Next we desire to find the rate at which j -particles pass through a plane inside (or on the edge of) the slab. Consider particles inside the system traveling in direction 1 or 2, at depth x , and at time t . As noted above, in time dt , each particle travels a distance $ds = vdt$. So we find that the number of j -particles that pass through the plane located at x in time interval $(t, t + dt)$ is equivalent to the number of particles located in the *spatial* interval $(x, x + vdt)$ at time t ,

and this is just $N_j(x, t)vdt$. Now we divide by dt to obtain:

$$vN_j(x, t) = \text{the rate that } j\text{-particles cross the plane at } x \text{ at time } t \quad (2.3)$$

The quantities defined in Equations (2.1), (2.2), and (2.3) are important and useful. Equation (2.1) tells us the number of particles in any specified volume at any time t . Equation (2.2) allows us to predict the collision rate in some volume at time t , and Equation (2.3) allows us to calculate the rate at which radiation crosses any surface at time t . It is not difficult to find applications where these quantities are useful; shielding and food/mail irradiation come to mind.

2.1.1 Model Derivation

To form the equations, our only remaining task is to create a balance equation relating these quantities. That is, if $N_j(x, t)dx$ is the number of j -particles in $(x + dx)$ at time t , then

$$\begin{aligned} \frac{\partial N_j}{\partial t}(x, t) &= \text{the rate of change of } j\text{-particles in } (x, x + dx) \text{ at time } t. \\ &= [\text{the rate of } \textit{gain} \text{ of } j\text{-particles in } (x, x + dx) \text{ at time } t] \\ &\quad - [\text{the rate of } \textit{loss} \text{ of } j\text{-particles in } (x, x + dx) \text{ at time } t] \quad . \end{aligned}$$

and these gain/loss terms are represented by:

$$\frac{\partial N_j}{\partial t}(x, t) = \left\{ \begin{array}{l} \text{[the rate that } j\text{-particles flow into } (x, x + dx) \text{ at time } t] \\ \end{array} \right. \quad (2.4a)$$

$$+ \left[\begin{array}{l} \text{the rate particles in } (x, x + dx) \text{ scatter to direction } j \text{ at time } t \\ \end{array} \right] \quad (2.4b)$$

$$+ \left. \begin{array}{l} \text{[the rate particles are born in } (x, x + dx), \text{ with direction } j \text{ at} \\ \text{time } t \text{ due to the inhomogenous source} \\ \end{array} \right\} \quad (2.4c)$$

$$- \left\{ \begin{array}{l} \text{[the rate that } j\text{-particles flow out of } (x, x + dx) \text{ at time } t] \\ \end{array} \right. \quad (2.4d)$$

$$+ \left. \begin{array}{l} \text{[the rate that } j\text{-particles in } (x, x + dx) \text{ undergo collisions} \\ \end{array} \right\} \quad (2.4e)$$

Each of the quantities in Equations (2.4) can be represented mathematically. To begin, we consider the quantity in Equation (2.4a), the rate that j -particles flow into the volume $(x + dx)$ at time t . For right-going particles, this is just the rate that particles enter the plane at x ; for left-going it is the rate for the plane at $x + dx$. Then, by Equation (2.3), this entrance rate is

$$= \left\{ \begin{array}{ll} vN_1(x, t), & j = 1 \\ vN_2(x + dx, t), & j = 2 \end{array} \right. \quad (2.5a)$$

Similarly the rate at which j -particles leave the volume $(x + dx)$ at time t [Equation (2.4b)] is given by the number that cross the outgoing plane. For right-going particles, this is just the rate that particles leave the plane at $x + dx$; for left-going

it is the rate for the plane at x . So this loss rate is

$$= \begin{cases} vN_1(x + dx, t), & j = 1 \\ vN_2(x, t), & j = 2 \end{cases} \quad (2.5b)$$

The source rate $\frac{1}{2}q(x, t)dx$ by definition is what is required for Equation (2.4c), the rate that particles are born in $(x + dx)$ in direction j at time t . The factor of $1/2$ arises since the source is isotropic. Equation (2.2) directly gives us the collision rate for j -particles in $(x, x + dx)$ at time t , required for Equation (2.4d). This rate is

$$= \Sigma_t v N_j(x, t) dx \quad (2.5c)$$

The only remaining term is Equation (2.4b), the rate at which particles in $(x + dx)$ scatter into direction j at time t . For this, let us first consider the collision rate of all the particles in this volume, given by $\Sigma_t v [N_1(x, t) + N_2(x, t)] dx$. Multiplying this quantity by the scattering ratio c , we obtain the scattering rate of all these particles $\Sigma_s v [N_1(x, t) + N_2(x, t)] dx$. Finally, we multiply this result by the probability a particle scatters into direction j ($1/2$, isotropic scattering) to obtain the rate at which particles scatter into direction j

$$= \frac{1}{2} \Sigma_s v [N_1(x, t) + N_2(x, t)] dx \quad (2.5d)$$

We have now come to a point where we can write the balance equation mathematically. Combining Equations (2.4) and (2.5) with the definition for the source

rate, we find that:

$$\begin{aligned} \frac{\partial N_j}{\partial t}(x, t) = & \left\{ \begin{array}{l} vN_1(x, t), \quad j = 1 \\ vN_2(x + dx, t), \quad j = 2 \end{array} \right\} + \frac{\Sigma_s}{2}v [N_1(x, t) + N_2(x, t)] dx \\ & + \frac{1}{2}q(x, t)dx - \left\{ \begin{array}{l} vN_1(x + dx, t), \quad j = 1 \\ vN_2(x, t), \quad j = 2 \end{array} \right\} - \Sigma_t v N_j(x, t) dx \end{aligned}$$

Rearranging, this is:

$$\begin{aligned} \frac{\partial N_j}{\partial t}(x, t) + v \left\{ \begin{array}{l} N_1(x + dx, t) - N_1(x, t), \quad j = 1 \\ N_2(x, t) - N_2(x + dx, t), \quad j = 2 \end{array} \right\} + \Sigma_t v N_j(x, t) dx \\ = \frac{\Sigma_s}{2}v [N_1(x, t) + N_2(x, t)] dx + \frac{1}{2}q(x, t)dx \quad (2.6) \end{aligned}$$

For the terms in the brackets, we can Taylor expand about x and (neglecting terms of order dx^2) we find

$$\begin{aligned} N_1(x + dx, t) - N_1(x, t) &= \frac{\partial N_1}{\partial x}(x, t)dx \\ &= \mu_1 \frac{\partial N_1}{\partial x}(x, t)dx \quad (2.7a) \end{aligned}$$

and

$$\begin{aligned} N_2(x, t) - N_2(x + dx, t) &= -\frac{\partial N_2}{\partial x}(x, t)dx \\ &= \mu_2 \frac{\partial N_2}{\partial x}(x, t)dx \quad (2.7b) \end{aligned}$$

where we have defined

$$\mu_j = \begin{cases} +1, & j = 1 \\ -1, & j = 2 \end{cases} = \underline{\Omega}_j \cdot \underline{i} \quad (2.8)$$

The quantity μ_j may be thought of the cosine of the angle of flight with respect to the x -axis. It just happens here that it is only allowed two values. Introducing Equations (2.7) and (2.8) into (2.6) and dividing through by dx , we find (for $j = 1, 2$):

$$\frac{\partial N_j}{\partial t}(x, t) + \mu_j v \frac{\partial N_j}{\partial x}(x, t) + \Sigma_t v N_j(x, t) = \frac{\Sigma_s}{2} v [N_1(x, t) + N_2(x, t)] + \frac{1}{2} q(x, t) \quad (2.9)$$

It is conventional to here define the new function

$$\psi_j(x, t) = v N_j(x, t) = \text{“angular flux”} \quad (2.10)$$

so that Equations (2.9) become

$$\frac{1}{v} \frac{\partial \psi_j}{\partial t}(x, t) + \mu_j \frac{\partial \psi_j}{\partial x}(x, t) + \Sigma_t \psi_j(x, t) = \frac{\Sigma_s}{2} [\psi_1(x, t) + \psi_2(x, t)] + \frac{1}{2} q(x, t) \quad (2.11)$$

This is the main result, but we are not quite done. To make the problem well-posed, we must derive boundary and initial conditions for this first-order, coupled, partial differential equation. But we have already defined the boundary source, so the boundary conditions are given by:

$$\left. \begin{aligned} \psi_1(0, t) &= \psi_1^b(t) \\ \psi_2(X, t) &= \psi_2^b(t) \end{aligned} \right\} 0 < t < \infty \quad (2.12)$$

Finally, in order to predict the angular fluxes $\psi_1(x, t)dx$ and $\psi_2(x, t)dx$ at any given time using only a physical model of particle interactions, we must be provided with the spatial distribution of both quantities at a point in time (initial conditions). We will denote these initial conditions as $\psi_1^i(x)$ and $\psi_2^i(x)$. So the initial conditions tell us that:

$$\psi_j(x, t_0) = \psi_j^i(x), \quad 0 < x < X \quad j = 1, 2 \quad (2.13)$$

Equations (2.11) with boundary conditions (2.12) and initial conditions (2.13) are a coupled, first-order partial differential system that provides one with a model to represent time- and space-dependent particle transport through a semi-infinite slab. Because most applications that employ this model require only the behavior of the interactions at steady-state, we may allow $\partial\psi_j(x, t)/\partial t \rightarrow 0$ to find the following system of coupled, first-order ordinary differential equations:

$$\mu_j \frac{d\psi_j}{dx}(x) + \Sigma_t \psi_j(x) = \frac{\Sigma_s}{2} [\psi_1(x) + \psi_2(x)] + \frac{q(x)}{2}, \quad (2.14a)$$

$$0 < x < X, \quad j = 1, 2.$$

$$\psi_1(0) = \psi_1^b, \quad (2.14b)$$

$$\psi_2(X) = \psi_2^b \quad (2.14c)$$

2.1.2 Discussion

The system given by Equations (2.14) is the focus of this thesis. Because of the assumptions made in developing the system, it is possible to find an exact solution, and therefore have an answer against which to compare the less exact

nature of the computational models developed below. However, some comments should be made about these assumptions with regard to their relevance. First, the above system may be thought of as an equation for the mean value of particles, whose variance may be considered small only if there are a large number of particles. That is, the above derivation is for a continuum model and effectively assumes the number of particles is infinite. Fortunately, in typical neutron problems, $N \approx 10^{14}$ neutrons/cc (which is large enough). But if the number of particles is not very large, this model may not be accurate. Also, in more realistic problems particles can travel in any direction and at different speeds, the cross sections may be space and energy dependent, and scattering need not be isotropic. However, this model contains a great deal of “truth.” Extensions of the model to accommodate these facts still leave its basic structure intact. Finally, it is noteworthy that a minor modification to this model to expand the directions of flight brings the model into agreement with the simplest practical model for neutron transport (the so-called S_2 model). In the S_2 model, we essentially replace $\mu_j = (-1)^{j+1}$ with $\mu_j = (-1)^{j+1}/\sqrt{3}$, meaning that particles are allowed to travel in any direction along a cone whose angle is approximately 54.7 degrees with the x -axis (in the left and right directions).

In the next chapter we will present the analytical solution of Equations (2.14).

2.2 Deterministic Modeling

In a deterministic approach, the problem geometry is typically split up (discretized) into many subintervals and Equations (2.14) are averaged over these intervals. One then assumes some relationship between the average quantities of adjacent cells, and guesses a solution in an attempt to satisfy the discretized

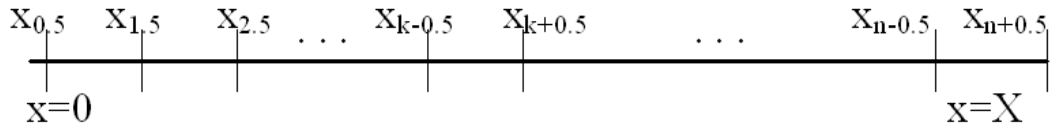


Figure 2.3: Discretization scheme for finite difference method

equations. This solution is then iterated upon until a suitable tolerance is met, at which point the simulation has finished. This approach has the advantage of being a relatively quick way to obtain global estimates of quantities of interest. Its main disadvantage is that, because of this averaging, the final result is subject to truncation errors; it is not exact. One only hopes that the deterministic solution is within some tolerance of the “real” solution. However, one can be sure that once all the parameters are chosen, this algorithm will always produce the same prediction (the prediction is *determined* by the choice of parameters).

For this problem we are employing a deterministic approach known as the finite difference method. First, we split up the region $0 < x < X$ into n subdomains of width Δx_k (the width of each cell may vary). Figure 2.3 illustrates this discretization. We then make the following definitions. As stated above, the distance between two gridpoints is given by

$$\Delta x_k = x_{k+0.5} - x_{k-0.5}. \quad (2.15a)$$

The inhomogenous source term will be averaged over the k -th interval:

$$q^k = \frac{1}{\Delta x_k} \int_{x_{k-0.5}}^{x_{k+0.5}} q(x) dx \quad (2.15b)$$

The values of ψ_j at the edges of the k -th interval are defined explicitly to be:

$$\psi_j^{k+0.5} = \psi_j(x_{k+0.5}) \quad (2.15c)$$

$$\psi_j^{k-0.5} = \psi_j(x_{k-0.5}) \quad (2.15d)$$

And the average value of ψ_j on the k -th interval is given by:

$$\psi_j^k = \frac{1}{\Delta x_k} \int_{x_{k-0.5}}^{x_{k+0.5}} \psi_j(x) dx \quad (2.15e)$$

Next we operate on the ODE in Equations (2.14) using $\frac{1}{\Delta x_k} \int_{x_{k-0.5}}^{x_{k+0.5}} (\cdot) dx$ to obtain, without approximation,

$$\begin{aligned} \frac{\mu_j}{\Delta x_k} \int_{x_{k-0.5}}^{x_{k+0.5}} \frac{d\psi_j}{dx}(x) dx + \frac{\Sigma_t}{\Delta x_k} \int_{x_{k-0.5}}^{x_{k+0.5}} \psi_j(x) dx \\ = \frac{1}{\Delta x_k} \int_{x_{k-0.5}}^{x_{k+0.5}} \left[\frac{\Sigma_s}{2} [\psi_1(x) + \psi_2(x)] + \frac{q(x)}{2} \right] dx, \end{aligned}$$

$$1 < k < n, \quad j = 1, 2.$$

Using the fundamental theorem of calculus on the differential term and the definitions in Equations (2.15), we obtain the following discretized system of equations and boundary conditions.

$$\mu_j \frac{\psi_j^{k+0.5} - \psi_j^{k-0.5}}{\Delta x_k} + \Sigma_t \psi_j^k = \frac{\Sigma_s}{2} [\psi_1^k + \psi_2^k] + \frac{q^k}{2}, \quad (2.16a)$$

$$1 < k < n, \quad j = 1, 2.$$

$$\psi_1^{0.5} = \psi_1^b, \quad (2.16b)$$

$$\psi_2^{n+0.5} = \psi_2^b \quad (2.16c)$$

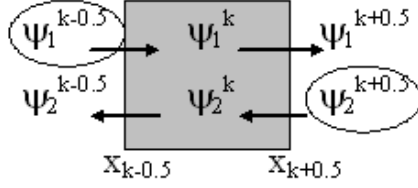


Figure 2.4: Illustration of knowns (circled) and unknowns for the k th interval

Equations (2.16) are a system such that, for each k -interval, there are 4 unknowns but only 2 equations. Figure 2.4 illustrates how this is so (if we counted 6 unknowns per cell, we would be double counting the cell edges). To close this system, we must add 2 equations per interval. This can be done by applying a finite differencing scheme, in which we assume some relationship between $\psi_j^{k-0.5}$, ψ_j^k , and $\psi_j^{k+0.5}$. For instance, one might choose to approximate the quantity ψ_j^k by averaging the edge values. For our model, we will use what is known as an *implicit* differencing scheme – we will assume that $\psi_1^{k+0.5} = \psi_1^k$ and $\psi_2^{k-0.5} = \psi_2^k$. Implicit differencing schemes are known to be more slowly converging than schemes that use both edge values but their advantage is that they are guaranteed to converge for most problems. So the first approximation we make is to insert $\psi_1^{k+0.5} = \psi_1^k$ into the first of Equations (2.16) to find

$$\begin{aligned}
\mu_1 \frac{\psi_1^{k+0.5} - \psi_1^{k-0.5}}{\Delta x_k} + \Sigma_t \psi_1^{k+0.5} &= \frac{\Sigma_s}{2} [\psi_1^{k+0.5} + \psi_2^k] + \frac{q^k}{2}, \\
\psi_1^{k+0.5} \left(\frac{\mu_1}{\Delta x_k} + \Sigma_t - \frac{\Sigma_s}{2} \right) &= \frac{\Sigma_s}{2} \psi_2^k + \frac{q^k}{2} + \frac{\mu_1}{\Delta x_k} \psi_1^{k-0.5}, \\
\psi_1^{k+0.5} &= \frac{\Delta x_k \Sigma_s \psi_2^k + \Delta x_k q^k + 2\mu_1 \psi_1^{k-0.5}}{2\mu_1 + 2\Delta x_k \Sigma_t - \Sigma_s \Delta x_k} \quad (2.17a)
\end{aligned}$$

Similarly, we substitute $\psi_2^{k-0.5} = \psi_2^k$ into the second of Equations (2.16) to find

$$\psi_2^{k-0.5} = \frac{\Delta x_k \Sigma_s \psi_2^k + \Delta x_k q^k - 2\mu_1 \psi_1^{k-0.5}}{-2\mu_2 + 2\Delta x_k \Sigma_t - \Sigma_s \Delta x_k} \quad (2.17b)$$

Equations (2.17), together with the two boundary conditions, provide a computational method to find the discretized solutions ψ_j^k . We first make an estimate of ψ_1^k and ψ_2^k for all points in the system; typically, we set all values to zero. The idea is to begin in a place at which particles are entering the system, the boundary for instance. So if particles are entering (say) the left side, we sweep from left to right, updating the values of $\psi_1^{k+0.5}$ using the first of Equations (2.17). Once we reach $k = n$, we sweep from right to left, updating $\psi_2^{k-0.5}$. At the end of each sweep, we compare the current results to the previous, and if they are all within a user-defined tolerance, the calculation is ended. This approach is also known as a “source iteration” procedure [2]. Essentially what is happening is that for each iteration, we are making an estimate of the right hand side of Equations (2.16), the source terms, and using it to update the flux. According to Reference [2], Equation (1.10), it is easy to show that the estimate of $\psi_j(x)$ after the n -th iteration is essentially the angular flux due to particles that have scattered at most $n - 1$ times. We therefore expect that an algorithm like this one is likely to converge quickly for systems in which little scattering occurs, like “leaky” or absorption-dominated systems (c small).

2.3 Stochastic Modeling

In a stochastic approach, no knowledge of the underlying equation is necessary; only knowledge of the underlying physical process is required. This is one of its

great advantages; there is no need to derive the above equations! Also, given enough time, one could theoretically simulate enough particles to find the exact solution to within a given amount of statistical error. Of course, the disadvantage to this method is that it takes much more time, as we shall see. Also, because random numbers are involved, this approach will not always produce the (exact) same prediction.

The essential idea behind this method is to follow many particles from their “birth” to their “death” by using probability distribution functions to determine what events they undergo. Let us imagine a problem in which particles enter the slab from the left. So, for our purposes, the particle is born at $x = 0$ with direction $\mu_1 = 1$. Once the particle enters the slab, there is an incremental probability of a collision per incremental distance given by Σ_t (and this is the only event that can occur inside the slab). So consider $\psi_u(x)$ to be the “uncollided” flux – the flux-quantity that is the sum of all particles that have not undergone a collision event. We may write:

$$\psi_u(x + \Delta x) = \psi(x) - \Sigma_t \Delta x \psi_u(x) + O(\Delta x^2) \quad (2.18)$$

which is to say, the uncollided flux at position $x + \Delta x$ is the uncollided flux at position x minus the amount that collided in Δx ($\Sigma_t \Delta x$ is the probability of a collision occurring in Δx). Particles that have collided more than once are in the $O(\Delta x^2)$ term. Rearranging this equation we have:

$$\frac{\psi_u(x + \Delta x) - \psi(x)}{\Delta x} = -\Sigma_t \psi_u(x) + O(\Delta x)$$

Allowing $\Delta x \rightarrow 0$, we find (by the definition of the derivative):

$$\frac{d\psi_u}{dx}(x) + \Sigma_t \psi_u(x) = 0$$

which we may solve to find that the uncollided flux is given by:

$$\psi_u(x) = C e^{-\Sigma_t x}$$

We integrate this equation from $x = 0$ to ∞ and set this equal to one to find the normalization constant for this probability distribution function:

$$\begin{aligned} \int_0^{\infty} C e^{-\Sigma_t x} dx &= 1, \\ -C \Sigma_t^{-1} e^{-\Sigma_t x} \Big|_0^{\infty} &= 1, \\ C &= \Sigma_t \end{aligned}$$

Therefore,

$$f(x) = \Sigma_t e^{-\Sigma_t x} \tag{2.19}$$

is the distribution we need to sample to determine the probability of a collision event in dx at depth x . However, most computer languages (such as Matlab, the one used in this thesis) use random number generators given by a uniform deviation between $(0, 1]$ (a uniform random deviate). So, to sample a collision

location from $f(x)$, we will use the cumulative distribution function:

$$\begin{aligned} F(x) &= \int_0^x f(x)dx, \\ &= 1 - e^{-\Sigma_t x}, \end{aligned}$$

We can solve this for x in terms of $F(x)$:

$$\begin{aligned} e^{-\Sigma_t x} &= 1 - F(x), \\ x &= -\Sigma_t^{-1} \ln(F(x) - 1) \end{aligned}$$

Since $F(x)$ varies uniformly from 0 to 1, it is simple to use a uniform random deviate to find x , the collision location, using this equation. So we replace $F(x) - 1$ with ξ_1 , some number determined from a uniform random number generator on $(0, 1]$ to find:

$$x = -\Sigma_t^{-1} \ln(\xi_1) \tag{2.20}$$

The hard part is over. Once we find the collision location, we test to see if the particle is still inside the slab. If it's not, we consider the particle history to be over. If it is, then we must determine what type of collision has occurred, an absorption or a scatter. For this we need only test to see if another uniform random deviate, ξ_2 is less than c . If it is, a scatter event has occurred, if not, an absorption event has occurred. Absorption events end the particle history, but if a scatter event occurs, we must sample using ξ_3 to determine which direction the particle has emerged in (we might assign the new direction to be “left” if $\xi_3 < 0.5$, “right” if $\xi_3 > 0.5$; scattering is isotropic). With this new particle position and direction, we may repeat the process of finding the collision location, collision

type, and new direction until the particle either leaves the system or is absorbed. A schematic of this process is shown in Figure 2.5.

As the particle history is carried out we may record the number of times any event of interest as occurred. At the end of the entire simulation (after many particles have been simulated), we can divide this number by the number of particles simulated to obtain an estimate of the average ratio of these event occurrences per incident particle. For instance, we could record the number of times a particle leaves the slab to the right to find an estimate of the average particle leakage to the right. So if y is some event of interest, we have the result

$$\hat{y} = \frac{1}{N} \sum_{n=1}^N y_n, \quad (2.21)$$

where \hat{y} is the *sample* mean of the events [3]. By the central limit theorem, if we sample enough particles, then the sample mean \hat{y} should converge to the true mean \bar{y} . Since we desire an exact solution, we are interested in knowing the probability that our estimate of the mean, \hat{y} is within some interval of \bar{y} . The quantity that gives us this information is the standard deviation of the sample mean $\sigma(\hat{y})$, which, roughly speaking, is the amount of uncertainty in our estimate \hat{y} . One can imagine that as the number of simulated particles is increased, the uncertainty will decrease. In fact it is shown in Reference [3], Equation (7.93) that

$$\sigma(\hat{y}) = \frac{\sigma(y)}{\sqrt{N}}, \quad (2.22)$$

where $\sigma(y)$ is the true standard deviation and N is the number of simulated particles. So our ability to measure the deviation in our estimate \hat{y} now hinges on our ability to estimate $\sigma(y)$. For this, it can be shown that the “sample

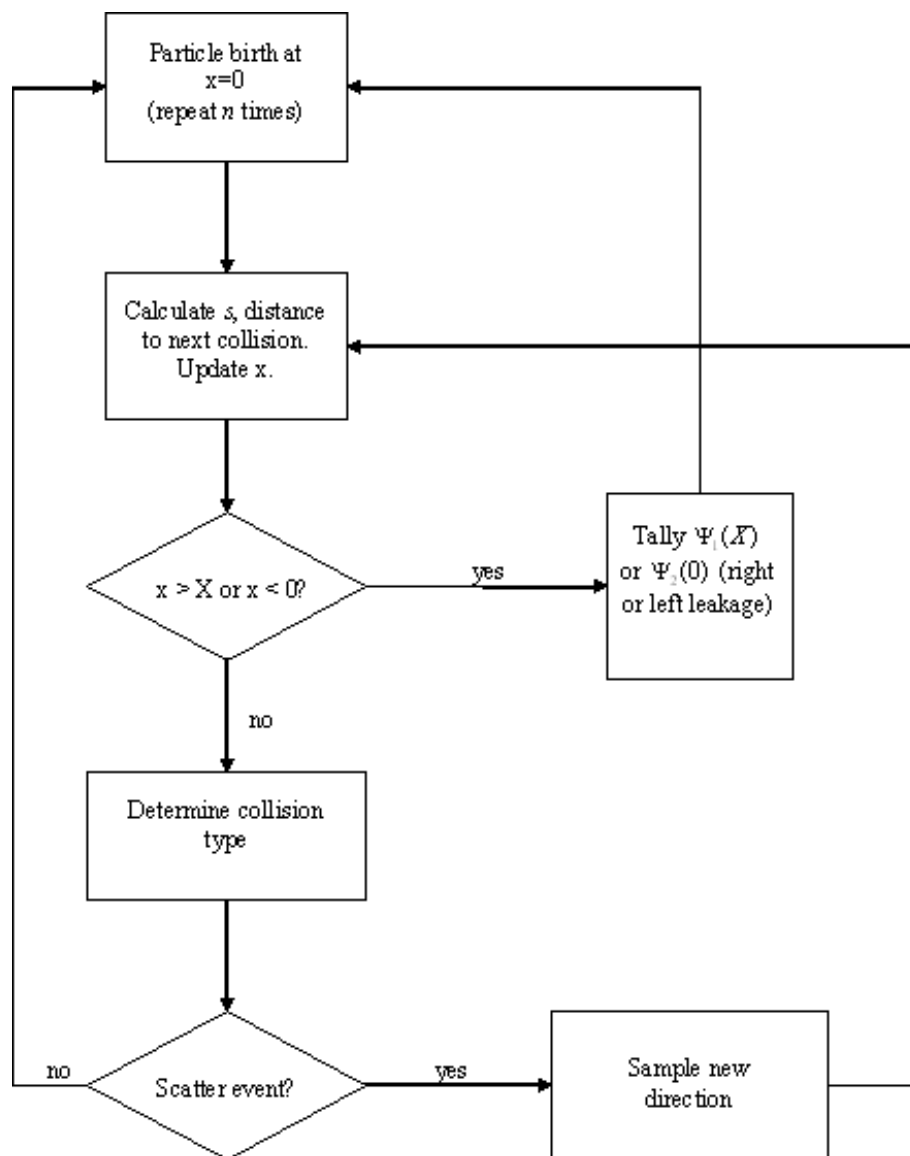


Figure 2.5: Flow chart of Monte Carlo algorithm

variance” S^2 may be used as an unbiased estimator of $\sigma^2(y)$, where

$$S^2 = \frac{1}{N-1} \sum_{n=1}^N (y_n - \hat{y})^2, \quad (2.23)$$

is the sample variance for N histories. Equation (2.23) may be rearranged to find that

$$S = \left(\frac{N}{N-1} \right)^{1/2} \left[\frac{1}{N} \sum_{n=1}^{\infty} y_n^2 - \left(\frac{1}{N} \sum_{n=1}^{\infty} y_n \right)^2 \right]^{1/2}, \quad (2.24)$$

This allows us to keep two running tallies (sums) to find the sample variance; in one we continually add y_n^2 , in the other we continually add y_n . So at the end of the simulation we use the y_n tally to find \hat{y} using Equation (2.21), and we use both the y_n and the y_n^2 tally to find S and obtain $\sigma(\hat{y}) = S/\sqrt{N}$ from Equation (2.22).

One of the drawbacks of an approach like this is that for every quantity of interest (e.g. particle leakage, flux through a plane) we must keep two running tallies whose statistics may converge at varying rates. For instance, if we consider a highly scattering problem (c near 1) and desire information about the flux distribution deep inside the slab, we must simulate many collision before we can tally a plane-crossing of interest. For this and other reasons, stochastic (Monte Carlo) methods are considered to be best suited for finding few, local results of interest. There has also been much research in ways to “push” the particles towards regions of interest in an unbiased way; these are known as non-analog methods. The method we have described above is strictly analogous to the underlying physics (an analog method), and this is what is implemented for this thesis.

Table 2.1: Parameters used for test problems

Parameter	Value(s)
Length X	10 cm
Σ_t	1 cm ⁻¹
c	0.1, 0.5, 0.99
$q(x)$	0
ψ_1^b	1
ψ_2^b	0

2.4 Test Problems

To compare the above methodologies, we will consider a problem one might encounter in a shielding, astrophysical, or food irradiation application. That is, we will consider a uniform beam of neutral particles entering the left side of the slab whose material properties are known, and attempt to find out the percentage of the radiation transmitted through the slab, the percentage reflected, and the percentage absorbed. For this we will use the parameters provided in Table 2.4. These values correspond to a homogenous, 10 cm slab with a beam of radiation incident on the left hand side of the slab and having no inhomogeneous source. We stipulate that the total cross section is 1 cm⁻¹, but vary the scattering ratio to show its effect on computing times and modeling capabilities. The quantities of interest to us are $\psi_1(X)$, and $\psi_2(0)$; it is these that may be used to calculate the percentages of particles transmitted, reflected, and absorbed.

Chapter 3

Results

In this chapter we derive the analytical solution to Equations (2.14) with parameters given in Table 2.4, namely, $q(x) = 0$, $\psi_1^b = 1$, $\psi_2^b = 0$. The results of the deterministic and stochastic approaches for the 3 values of the scattering ratio will then be compared against the analytical solution for accuracy.

3.1 Analytical Solution

For this test problem, Equations (2.14) simplify to:

$$\frac{d\psi_1}{dx}(x) + \Sigma_t \psi_1(x) = \frac{\Sigma_s}{2} [\psi_1(x) + \psi_2(x)] \quad (3.1a)$$

$$-\frac{d\psi_2}{dx}(x) + \Sigma_t \psi_2(x) = \frac{\Sigma_s}{2} [\psi_1(x) + \psi_2(x)] \quad (3.1b)$$

with boundary conditions

$$\psi_1(0) = 1 \quad (3.1c)$$

$$\psi_2(X) = 0 \quad (3.1d)$$

We may rewrite these equations as:

$$\begin{aligned}\frac{d\psi_1}{dx}(x) &= \left(\frac{\Sigma_s}{2} - \Sigma_t\right)\psi_1(x) + \frac{\Sigma_s}{2}\psi_2(x) \\ \frac{d\psi_2}{dx}(x) &= -\frac{\Sigma_s}{2}\psi_1(x) + \left(\Sigma_t - \frac{\Sigma_s}{2}\right)\psi_2(x)\end{aligned}$$

If we define $a = \Sigma_t - \Sigma_s/2$, $b = \Sigma_s/2$, then this is:

$$\underline{\psi}' = \mathbf{A}\underline{\psi} \tag{3.2a}$$

where

$$\mathbf{A} = \begin{bmatrix} -a & b \\ -b & a \end{bmatrix}, \tag{3.2b}$$

$$\underline{\psi} = \begin{bmatrix} \psi_1(x) \\ \psi_2(x) \end{bmatrix} \tag{3.2c}$$

Equation (3.2a) is a homogeneous, linear system of first order ordinary differential equations. If $\Sigma_s \neq 0$ and $\Sigma_t \neq 0$ (which we assume here), then this amounts to an eigenvalue problem. The eigenvalues of \mathbf{A} are given by:

$$(-a - \lambda)(a - \lambda) + b^2 = 0,$$

$$\lambda^2 - a^2 + b^2 = 0,$$

$$\lambda^2 = a^2 - b^2,$$

$$\lambda = \pm \sqrt{\Sigma_t^2 - \Sigma_t \Sigma_s + \left(\frac{\Sigma_s}{2}\right)^2 - \left(\frac{\Sigma_s}{2}\right)^2},$$

$$\lambda = \pm \sqrt{\Sigma_t(\Sigma_t - \Sigma_s)}$$

If we define the ‘‘absorption’’ cross section to be $\Sigma_a = \Sigma_t - \Sigma_s$, then $\lambda = \pm\sqrt{\Sigma_t\Sigma_a}$.

Using these eigenvalues, the eigenvectors are found to be:

$$v_1 = \begin{bmatrix} 1 \\ \frac{b}{a-\sqrt{a^2-b^2}} \end{bmatrix}, v_2 = \begin{bmatrix} 1 \\ \frac{b}{\sqrt{a^2-b^2}+a} \end{bmatrix}$$

which is

$$v_1 = \begin{bmatrix} 1 \\ \frac{\Sigma_s/2}{\Sigma_t - \Sigma_s/2 - \sqrt{\Sigma_t\Sigma_a}} \end{bmatrix}, v_2 = \begin{bmatrix} 1 \\ \frac{\Sigma_s/2}{\sqrt{\Sigma_t\Sigma_a} + \Sigma_t - \Sigma_s/2} \end{bmatrix} \quad (3.3)$$

where v_1 is associated with the positive value of λ . Putting this together, we get the general solution to be:

$$\psi_1(x) = C_1 e^{\Sigma_t \Sigma_a x} + C_2 e^{-\Sigma_t \Sigma_a x}, \quad (3.4a)$$

$$\psi_2(x) = \frac{C_1 \Sigma_s/2}{\Sigma_t - \Sigma_s/2 - \sqrt{\Sigma_t \Sigma_a}} e^{\Sigma_t \Sigma_a x} + \frac{C_2 \Sigma_s/2}{\sqrt{\Sigma_t \Sigma_a} + \Sigma_t - \Sigma_s/2} e^{-\Sigma_t \Sigma_a x} \quad (3.4b)$$

Using the mathematical package Maple, we substitute the boundary conditions $\psi_1(0) = 1$ and $\psi_2(X) = 0$ to obtain the following analytical solution:

$$\psi_1(x) = \frac{(2\sqrt{\Sigma_t \Sigma_a} - 2\Sigma_t + \Sigma_s)e^{\sqrt{\Sigma_t \Sigma_a} x} + (2\sqrt{\Sigma_t \Sigma_a} + 2\Sigma_t - \Sigma_s)e^{\sqrt{\Sigma_t \Sigma_a}(2X-x)}}{2\sqrt{\Sigma_t \Sigma_a} - 2\Sigma_t + \Sigma_s + (2\sqrt{\Sigma_t \Sigma_a} + 2\Sigma_t - \Sigma_s)e^{2\sqrt{\Sigma_t \Sigma_a} X}} \quad (3.5a)$$

$$\psi_2(x) = \frac{-\Sigma_s \left(e^{\sqrt{\Sigma_t \Sigma_a} x} - e^{\sqrt{\Sigma_t \Sigma_a}(2X-x)} \right)}{2\sqrt{\Sigma_t \Sigma_a} - 2\Sigma_t + \Sigma_s + (2\sqrt{\Sigma_t \Sigma_a} + 2\Sigma_t - \Sigma_s)e^{2\sqrt{\Sigma_t \Sigma_a} X}} \quad (3.5b)$$

It is reaffirming to note that these equations agree with what one would expect. For instance, if $\Sigma_s \approx 0$, then $\psi_2(x)$ is nearly 0. This makes sense since the only source term for $\psi_2(x)$ arises from scattering from $\psi_1(x)$ (If particles are

Table 3.1: Analytical solutions for the test problem

c	0.10	0.50	0.99
Percentage Transmitted	0.00757913	0.082432	13.37283
Percentage Reflected	2.63340	17.15728	77.79306
Percentage Absorbed	97.35902	82.76029	8.83410

only absorbed, none scatter back). Also, $\psi_1(x)$ then becomes a purely decreasing exponential of the form $Ce^{-\Sigma_a x}$. Equations (3.5) are the solutions to which we'll hold the deterministic and stochastic approaches accountable. One might note that despite the simplicity of the assumptions involved in obtaining this solution, it is not trivial.

Finally, the pertinent data for the three scattering ratios is presented in Table 3.1. Recall that we desired the percentages of radiation reflected (given by $\psi_2(0)$), transmitted (given by $\psi_1(10)$), and the amount absorbed ($1-\psi_2(0) - \psi_1(10)$). These solutions agree with intuition; as the scattering ratio is increased, less particles are absorbed so, for a constant Σ_t , more particles are reflected and transmitted.

3.2 Data Analysis

For this section we will first present the solutions predicted by the deterministic method followed by a short interpretation of the results. Following that is the predictions of the stochastic method and a discussion.

Table 3.2: Results of the deterministic solutions for the test problem

c	0.10	0.50	0.99
% Error Transmitted	122.840	62.2258	5.9863
% Error Reflected	-2.28×10^{-6}	-1.14×10^{-4}	-0.5797
% Error Absorbed	-0.0096	-0.062	-3.9572
Required iterations	4	9	45
Processing time, s	0.46	0.46	0.48

3.2.1 Finite Difference

The results for the three cases are presented in Table 3.2.1. For each of these problems, the user-supplied tolerance was set to be 1×10^{-6} , and the mesh spacing is 0.2 cm. The large errors in the percentage of particles transmitted for the smaller c is a little misleading since this number is so small (see Table 3.1). However, in general it may be seen that the errors are increasing as c approaches one, and more iterations are required for convergence. This is expected as discussed above since each iteration represents (loosely) the number of collisions that occur for the angular flux. As for the processing times, they are all similar; this method predicts solutions fairly rapidly. Another advantage to this method is, after performing the simulation, we obtain results for the entire slab. Figures 3.1 through 3.3 depict the analytical and finite difference solutions for these three test problems. These figures depict how the nearly exponential decrease changes into a roughly linear decrease as c approaches 1, and also illustrates where the finite difference method has trouble converging – near places where the true solution is rapidly changing. Making Δx smaller helps to remedy this last effect.

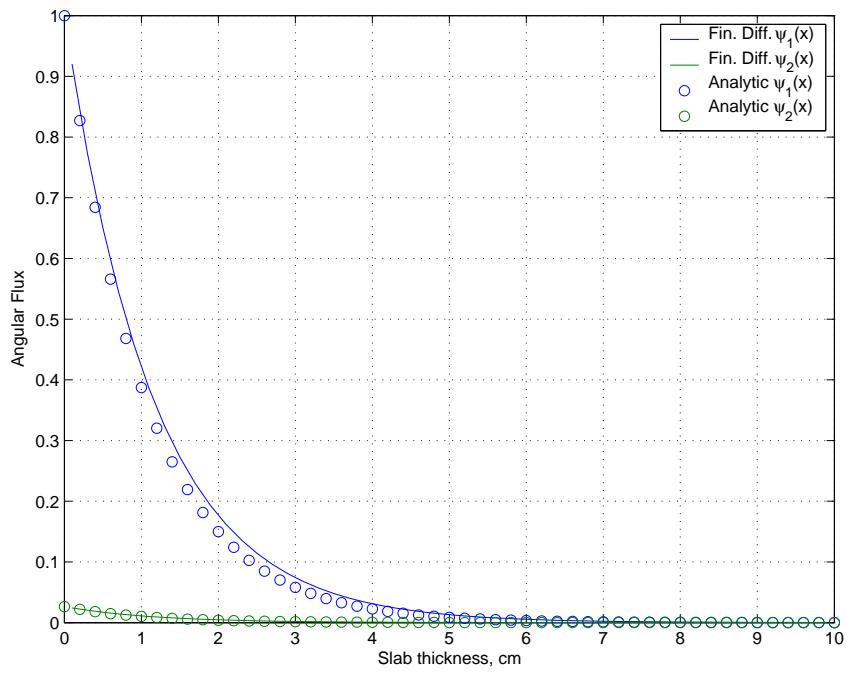


Figure 3.1: Test problem, $c = 0.1$

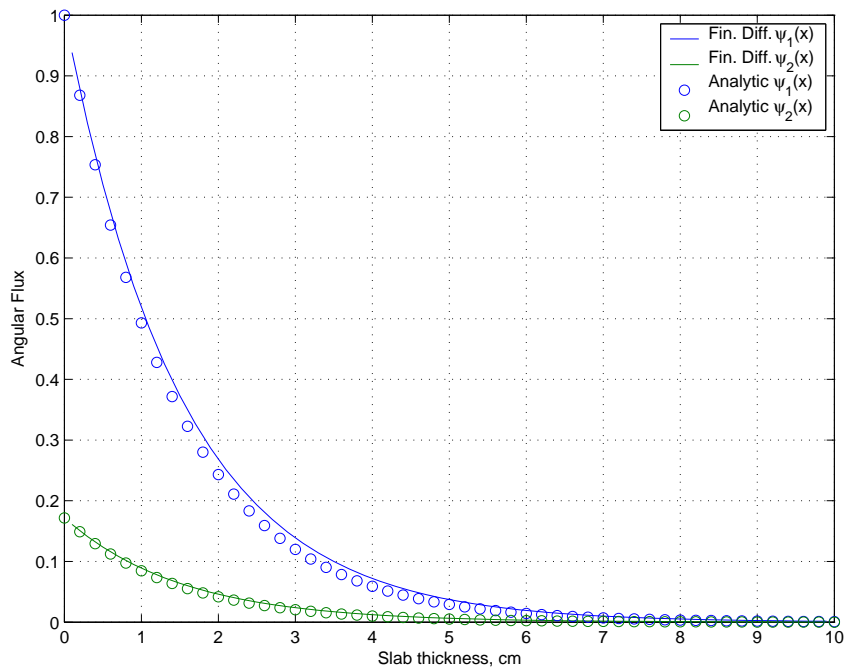


Figure 3.2: Test problem, $c = 0.5$

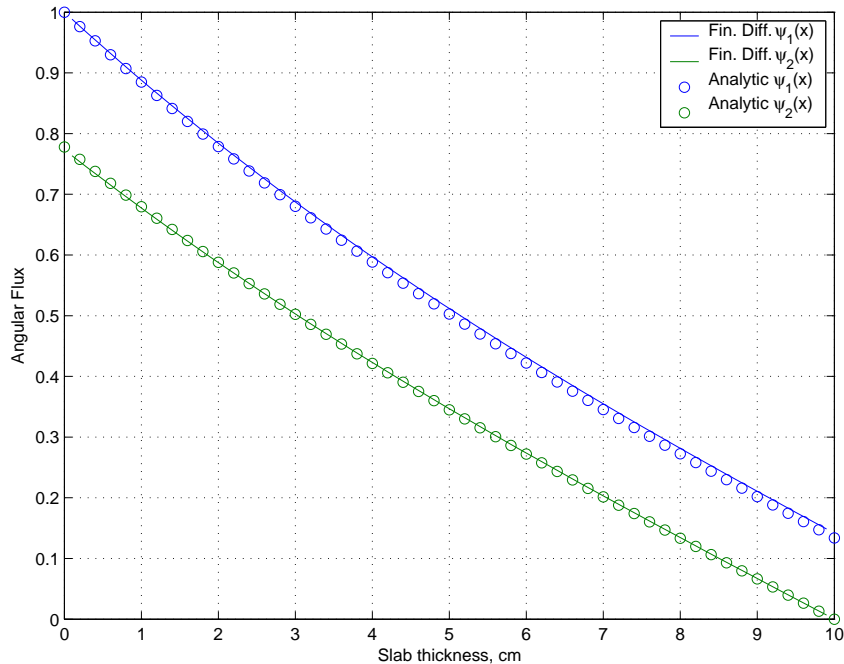


Figure 3.3: Test problem, $c = 0.99$

3.2.2 Monte Carlo

For the stochastic algorithm, in each test problem one million particle histories were simulated. The results in terms of percent error from the analytical solution are shown in Table 3.2.2. This table's most noticeable feature is the dramatic increase in computing time that occurs when c approaches unity. This is because when scattering increases almost every particle will die via leakage, so each must be followed for a longer time. The largest percent error that occurs is for the transmitted radiation when c is small; it is about 13%. This is not surprising since we would expect that the tally in that region did not receive very many accumulations due to particle events. Aside from this, though, most of the percentage errors are quite small.

Table 3.2.2 gives a measure of the statistical accuracy of the results; it shows

Table 3.3: Results of the Monte Carlo solutions for the test problem

c	0.10	0.50	0.99
% Error Transmitted	-12.9188	-3.6786	0.5449
% Error Reflected	-1.2343	-0.1584	0.0045
% Error Absorbed	0.0344	-0.0365	-0.8649
Processing time, s	28.2	49.6	291.24

Table 3.4: Statistical accuracy of the Monte Carlo solutions for the test problem

c	0.10		0.50		0.99	
In the bounds of?	σ	2σ	σ	2σ	σ	2σ
% Error Transmitted	no	yes	no	yes	no	yes
% Error Reflected	no	no	yes	yes	yes	yes
% Error Absorbed	no	yes	yes	yes	yes	yes

which predictions are within one and two standard deviations from the analytical solution. It turns out that 4 out of 9 of the results are within one standard deviation, and 8 out of 9 are within two standard deviations. This seems about right; for a Gaussian distribution, 67% of the time the answer is within one standard deviation, and 95% of the time it is within two deviations. It should be noted that the largest standard deviation in a result was only about a tenth of a percent of the total radiation modeled, and this occurred in the estimate of the radiation absorbed for $c = 0.99$.

Of course, increasing the number of histories will improve these estimates, but it takes a factor of 100 to decrease the error by a factor of 10. Looking at the numerical results, we may assess that, while the Monte Carlo method takes longer to produce answers, we have a higher degree of confidence in their accuracy.

Chapter 4

Conclusions

In this thesis we derived from first principles a simple transport model for radiation penetrating through a physical system and interacting with atoms within the system. We then discretized the system of equations and made some approximations that allowed us to create a deterministic algorithm that enables us to find solutions to the equations averaged over each interval. Also, from first principles and using probability density functions, a stochastic/Monte Carlo algorithm was derived to simulate individual particles travelling through the system to obtain ensemble-averaged results.

Next, three test problems were considered to illustrate the abilities of the two computational approaches. The parameters in the test problem were chosen so that the transport model could be solved exactly. This allowed us to directly assess the quality of the approximate solutions. For the three test problems, all quantities were fixed except for the scattering ratio, which varied from 0.1 to 0.5 to 0.99. We found that the finite difference (deterministic) approach was able to quickly achieve approximate results, but that the error increased when the spatial mesh sizes were increased or when the scattering ratio approached unity.

The Monte Carlo solutions were able to predict more accurate solutions, but this came at the expense of simulation time. Monte Carlo results took up to 600 times longer than the deterministic results, although our confidence in their accuracy was higher.

In summary, we found that both deterministic and stochastic methods are useful in simulating particle transport, and that they each have their own advantages and disadvantages. There is a considerable amount of research now in the development of “hybrid” methods, which attempt to use the best of both methods. The ideal method would work quickly and still be expected to provide an exact solution. Next year I will have the chance to research hybrid methods when I continue my education at the Masters level.

Bibliography

- [1] Wyatt D. Sharp and Edward J. Allen. “Stochastic Neutron Transport Equations for Rod and Plane Geometries”. *Annals of Nuclear Energy*, 27:99–116, 2000.
- [2] Marvin L. Adams and Edward W. Larsen. “Fast Iterative Methods for Discrete Ordinates Particle Transport Calculations”. *Progress in Nuclear Energy*, 40:3–159, 2002.
- [3] E.E. Lewis and W.F. Miller Jr. *Computational Methods of Neutron Transport*. John Wiley and Sons, New York, 1984.